

Physical modeling of fire tornados

A.M. Grishin,¹ A.N. Golovanov,¹ Ya.V. Sukov,¹ and R.Sh. Tsvyk²

¹*Tomsk State University*

²*V.E. Zuev Institute of Atmospheric Optics,
Siberian Branch of the Russian Academy of Sciences, Tomsk*

Received April 14, 2008

Fire tornados were generated under laboratory conditions by three independent ways. Similarity criteria for the problem of their generation were found. Formation of fire tornados is shown to not depend on the combustion source; it is determined by the heat flow density.

Introduction

Fire tornados, as a rule, arise in spacious urban¹ or forest^{2,19} fires. Of great interest are results of numerical simulation of the flame dynamics, fire whirls and tornados in the open space.³ At present, data on appearance and evolution of fire tornados are almost unavailable in literature, in contrast to atmospheric tornados.⁴

Powerful natural tornados arise from a rotating mother cloud and descend to the ground in the form of a proboscis. The rotational velocity at the periphery can reach sound velocity, and the centrifugal force creates a lower pressure inside the tornado. A fire tornado is a more complex physical phenomenon. It differs from usual atmospheric tornados by powerful intake of an oxidizer (air) into the combustion zone, which is necessary for burning the combustibles. Its features are a high temperature in the combustion zone due to chemical reactions of oxidation evolving a huge energy into rather large volume, and a powerful thermal convective column arising over the burning material. These features can change the conditions of a vortex flow appearance and similarity criteria, which describe such flows.

The most complete review of the experimental study of vortex flows is presented by T. Maxworthy.⁴ As a rule, in experiments the flow was swirled by walls and faces mounted around the excited domain, and the flow was developed in such bounded volume. The tangential swirling of liquid or gas through slots in the wall of the cylindrical chamber provides most stable vortex formations due to an additional pressure gradient, directed from the wall to the symmetry axis. However, this way has some disadvantages, because the role of radial movement of the gas mass to the tornado from the environment and a possibility of simulating such formations in an open space remains an enigma. An original way to obtain a vapor tornado is described by B.A. Lugovtsov.⁴

Whirlwinds of the tornado type were studied in Refs. 5–7 within the framework of the model of an ideal incompressible non-reacting liquid. A comprehensive introduction to the theory of concentrated vortices is given in Ref. 8.

A thermal whirlwind, arising over a rotating heated surface was experimentally studied in Ref. 9. It was proved that a stable vortex structure of the tornado type can appear at a certain rotational speed of the heated surface.

Of great interest are the techniques and results of the experimental study of spontaneous vortex structures in flames arising at combustion of hydrocarbon fuels in tubes and closed spaces.¹⁰

Analytical formulas for the height of a fire tornado were obtained^{11–13} in the framework of the model of a compressible multi-component ideal gas with the use of the hypothesis about local equilibrium of the rotating platform and the fire tornado.

The papers^{14–18} present the results of experimental studies of formation of the fire tornados by swirling an external air flow and the propagation of laser radiation through them. This way of tornado formation simulates flame swirling by atmospheric tornados, which arise near the Earth's surface, i.e., some analog of a boundary (tube) arises around the combustion source, which favors stabilization of the fire tornado. As it was shown,^{14–18} the stable fire tornado begins to form at the rotation speed $n > 2$ r/s and exists in fact until total burning out of the combustibles at the rotational speed of 18 r/s, that was recorded in the experiment. The height, diameter, effective heat flow of the fire tornado, fuel combustion rate, maximal frequency of the spectral function describing fluctuations of the gravity center of the image of the laser beam, propagating through the fire tornado, grow linearly with increase of the rotational speed at $n > 2$ r/s. The maximal frequency of the spectral function of intensity fluctuations grows linearly at $n > 5$ r/s. These characteristics (with allowance for the transition zone of fire tornado setting) can be well described for all n by an equation of the form $a + bn + c \exp(-n/k)$, where a , b , c , k are constants depending on the measured parameter. The linear dependence between the frequency, at which the maximum of fluctuations of the laser beam parameters is reached, and the rotation speed allow development of optical (remote)

methods for measuring the turbulent regime and components of flow velocity directly in the fire tornado.

Note that disadvantages are inherent to all ways of recording parameters of gas and liquid flow in vortex tornados. It is well-known that contact methods distort the structure of gas flows, and contactless ways of visualizing the hydrodynamic pattern of a flow in a vortex pose a problem of spatial-temporal resolution of flow lines. Optical methods, based on analysis of statistical parameters of laser beams, passed through a random medium, are widely used in atmospheric studies and for measuring parameters of the medium itself. Joint use of different methods for measurements of flow parameters by contact detectors and optical methods makes it possible to improve reliability of measurements and to develop new remote tools for measuring parameters of such a structurally complex medium in the fire tornado.

The goal of our work is to study conditions, under which fire tornados can appear and exist in the open space, as well as to compare fire tornados generated at burning of different combustibles, to determine significant similarity criteria and conditions of their appearance and existence. In this paper the fire tornado is simulated, which is formed due to vortex structures arising at rotation of the burning source.¹⁰ Investigation of conditions of appearance and determination of dimensionless similarity criteria, which describe hydrodynamic and thermal phenomena in similar structures of different sizes make it possible to use results of model experiments in the study of actual fire tornados. The developed passive (by statistical parameters of proper radiation of a flame) and active (with the use of radiation sources) optical methods for measuring parameters of a medium can be applied in large-scale models.

1. Combustibles

Model fire tornados were formed by combustion of: raw oil (simulation of an accident at oil storage tanks), forest combustibles (soil covered by dead leaves from pine, cedar for modeling forest fires), fragments of wooden buildings (large-scale and small-scale for simulation of fire tornados arising in large fires in forests, towns, and settlements).

Irregularity of the combustion surface was characterized by the following parameters (All-Union State Standard (GOST) 2.789-73): arithmetic mean deviation of the profile R_a , maximum arithmetic mean deviation of the profile R_z , R_{zn} , relative reference length t_a :

$$R_a = \frac{1}{N} \left(\sum_{i=1}^N |h_i - \langle h \rangle| \right),$$

$$R_z = \frac{1}{10} \left(\sum_{i=1}^{10} |h_{i_{\max}} - \langle h \rangle| + \sum_{i=1}^{10} |h_{i_{\min}} - \langle h \rangle| \right), \quad t_a = \frac{1}{l} \sum_{i=1}^n b_i,$$

where h_i is the height of irregularities; $\langle h \rangle$, $h_{i_{\max}}$, $h_{i_{\min}}$ are average, 10 maximal, and 10 minimal heights of irregularities; l is the total length of the analyzed path; b_i is the length of the path in irregularities at the level $\langle h \rangle$.

To compare parameters of irregularity in actual and model conditions, we compute the normalized deviation of the profile $R = R_a / \langle h \rangle$ and relative reference length t_a .

For small-scale fragments of wooden buildings, the dimensions in real conditions are as follows: $6 \times 5 \times 18$ m, the distance between fragments is 6 m, the parameter $\langle h \rangle = 3$ m, $R_a = 3$ m, $R = 1$, $t_a = 1$. The model dimensions (cut matches free of heads) are $(1 \times 1 \times 3) \cdot 10^{-3}$ m, the distance between the matches is 10^{-3} m, the parameter $\langle h \rangle = 5 \cdot 10^{-3}$ m, $R_a = 5 \cdot 10^{-3}$ m, $R = 1$, $t_a = 1$. For large-scale constructions (match boxes), parameters of irregularity are similarly close: $(10 \times 30 \times 50) \cdot 10^{-3}$ m.

Forest combustibles (FC) had the following dimensions: the effective diameter $D_+ = (0.5 \div 1.5) \cdot 10^{-3}$ m and length $l = (1 \div 5.0) \cdot 10^{-3}$ m, the thickness of a layer was ~ 0.02 m. Their moisture content $W = (m - m_0) / m_0 = 0.07 \div 0.13$, that is lower than the critical level, at which forest fires can arise.² Here m is the mass of moist fragments; m_0 is the mass of fragments dried at 373 K.

All the combustibles were placed on special bases and fired. The diameter of the bases varied from 0.06 to 0.35 m and coincided with the diameter of the combustion zone.

2. Experimental blocks and measurement techniques

Figure 1 presents the schemes of units providing different ways of swirling the fire tornados.

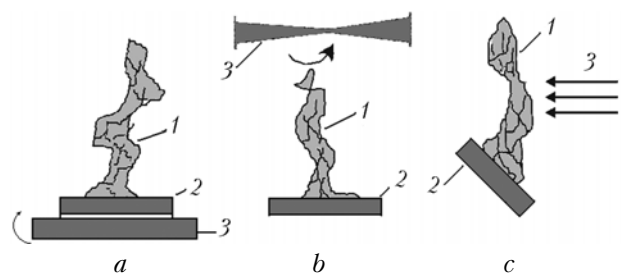


Fig. 1. Ways of modeling fire tornados.

Figure 1a shows a tangential swirling of a fire tornado 1, formed by combustibles on base 2, by rotation of the construction base 3 with the frequency f . Figure 1b demonstrates generation of a fire tornado 1 from combustibles placed on base 2, by rotation of fan blades 3 in the top of the torch. The base with the combustibles was stationary in this case. In Fig. 1c the fire tornado 1 is swirled by an air flow 3 which is generated by a subsonic wind tube of the type MT-324 in the direction perpendicular to the

torch symmetry axis. Base 2 with combustible materials is placed at an angle with respect to the vector of air flow velocity.

The following parameters of the fire tornado were determined in the experiments:

– gas temperature T_0 at the fire tornado axis was determined by the thermoelectrical method by the use of a Chromel-Alumel thermocouple with a junction diameter of $2 \cdot 10^{-4}$ m;

– heat flow density q was determined by the exponential method with a heat flow detector attached to a heat-insulated handle and made of a material with a high specific heat conductivity (copper of $2 \cdot 10^{-2}$ m in diameter), with a thermocouple of $2 \cdot 10^{-3}$ m in diameter mounted within it;

– the vertical V_z and tangential V_τ components of the flow rate were determined by the pneumometric method by the use of a Pitot tube of $2 \cdot 10^{-3}$ m in diameter (the method is based on measuring the difference of pressure towards the flow and perpendicularly to it), and by photographing trajectories of finely divided aluminum particles, which were added to the flow in the direction of the tangential velocity of the vortex rotation.¹⁰ Exposition time of the photographing was $\tau = 0.008$ sec;

– radial velocity of gas V_r in the space surrounding the fire tornado was determined by the hotwire method with a platinum filament of $2 \cdot 10^{-5}$ m in diameter and $6 \cdot 10^{-3}$ m in length;

– geometric dimensions: radius r and the maximum height h_c were determined by photographing the fire tornado. The film was processed at the microphotometer MP-2.

Total errors in determination of the parameters were: $\delta T \leq 5\%$, $\delta q \leq 9\%$, $\delta V \leq 9\%$ (hotwire), $\delta V \leq 8\%$ (tracks of luminescent particles), $\delta V \leq 6\%$ (Pitot nozzle), $\delta m \leq 2.5\%$ (weighting error). By results of measurements (3–5 experiments), confidence intervals were calculated with a confidence probability of 95%.

3. Results of the experiments

Figure 2 shows oil combustion in different regimes. The photos permit one to determine radius of the fire tornado and its height. When the mixture

of gaseous pyrolysis products of the combustibles (oil, FCM, and timber) with air is burning, a convective column is formed. The trajectories of motion inside the column have the form of helical curves. Therefore, this vortex flow can be considered as a model of a fire tornado.

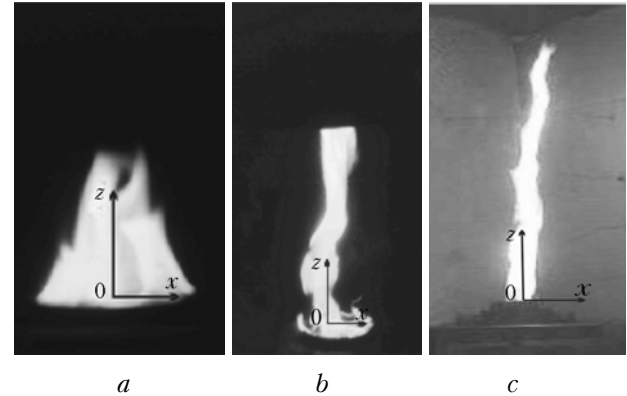


Fig. 2. Combustion of oil in the regime of diffusion fire: without swirling (*a*); with swirling of air from above (*b*); due to rotation of the base of the reservoir with fuel (*c*) at a rotational frequency of 1.3 Hz.

Table 1 presents the values of heat flow density q measured by a detector which was placed into different parts z of the combustion zone x , (see Fig. 2). The sensor is oriented in the direction of the z axis (the direction of velocity V_z). The detector was mounted on the axis of the fire tornado ($x = 0$), where q is maximal, and, for comparison, at the periphery of the fire tornado for $x = (3 \div 3.5) \cdot 10^{-2}$ m.

Analysis of the measurement results on heat flow density shows the flow to weakly depend on the type of combustibles. Their small-scale and large-scale fragments were made of pine, and the forest combustibles consisted of fallen leaves and needles of pine, cedar, and spruce.

The heat flow density in the fire tornado is by 13% higher than of the heat flow density from the freely burning surface. This can be explained by an increase of the convective component of the heat flow at formation of the fire tornado.

Table 1. Heat flow density when simulating the combustible firing in different regimes

| Type of the unit | Combustibles | q , 10^5 W/m ² | Coordinates, m | f , Hz |
|---------------------------|---------------------|-------------------------------|--|----------|
| Swirling of the base | Oil | 0.19 | $x = 3.0 \cdot 10^{-2}$, $z = 8.0 \cdot 10^{-2}$ | 1.1 |
| | Oil | 2.4 | $x = 0$, $z = 0.2 \cdot 10^{-2}$ | 1.3 |
| | Fragments: | | | |
| | Large-scale | 0.34 | $x = 3.5 \cdot 10^{-2}$, $z = 16.5 \cdot 10^{-2}$ | 1.3 |
| | Small-scale | 1.91 | $x = 0$, $z = 0.2 \cdot 10^{-2}$ | 1.2 |
| Swirling from above | Oil | 2.3 | $x = 0$, $z = 0.2 \cdot 10^{-2}$ | 1.1 |
| | Forest combustibles | 2.1 | $x = 0$, $z = 0.2 \cdot 10^{-2}$ | 1.2 |
| Base in a horizontal flow | Oil | 2.0 | $x = 0$, $z = 0.2 \cdot 10^{-2}$ | 1.2 |
| | Forest combustibles | 2.2 | $x = 0$, $z = 0.2 \cdot 10^{-2}$ | 1.1 |

Table 2 presents the values of heat flow density q and burning rate m_b for oil, calculated from the mass m and the burning time τ_0 .

Table 2. Calculated values of heat flow density q in a fire tornado during burning of oil

| $m, 10^{-3} \text{ kg}$ | $\tau_0, \text{ sec}$ | $M_b, \text{ g/sec}$ | $q, 10^5 \text{ W/m}^2$ | A | $f, \text{ Hz}$ |
|-------------------------|-----------------------|----------------------|-------------------------|------|-----------------|
| 18.3 | 278 | 0.066 | 1.9 | 0.67 | 1.1 |
| 31.7 | 473 | 0.067 | 2.4 | 0.70 | 1.2 |
| 32.0 | 406 | 0.079 | 2.3 | 0.65 | 1.2 |

The heat flow density was calculated by the formula

$$q = AmQ_+/\tau_0S,$$

where $Q_+ = 46 \cdot 10^6 \text{ J/kg}$ is the thermal efficiency of oil combustion; S is the area of the burning surface; A is a matching factor, which is introduced to take into account non-controlled heat losses for radiation and transfer by convective flows arising at the boundary of combustion. It is seen that the density of heat flows, generated by fire tornados in laboratory conditions, agrees with the calculated data (see Tables 1 and 2).

Table 3 presents the values of gas flow velocity components measured by different ways. Coordinates of measurement points were chosen in such a way for to clear up the mechanism of fire tornado formation, the role of gas swirling and its inflow from the surrounding space to the fire tornado. In the experiments, a radial inflow of air in the lower part of the fire tornado was observed. This proves the fact that the combustion process in the fire tornado is maintained by an oxidizer inflow from the surrounding medium, which corresponds to the diffusion mode of the combustion.

Figure 3 presents the tangential component V_τ as a function of coordinates. The dashed line shows the average radius of the fire tornado (see the data in Table 6 below). As follows from Fig. 3, at $z > 0.04 \text{ m}$, the component V_τ is almost constant in height inside the fire tornado, grows to its periphery, and rapidly decreases beyond it.

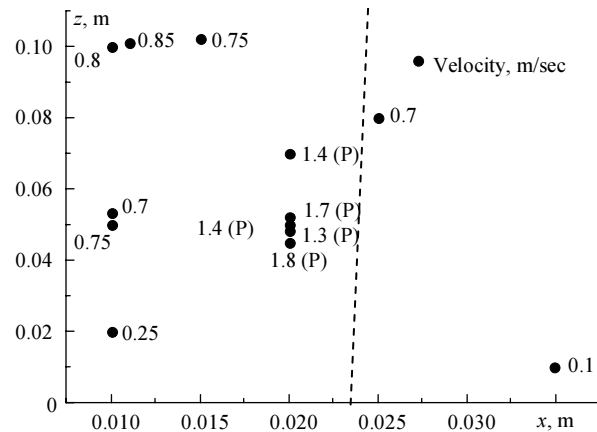


Fig. 3. The tangential component V_τ as a function of coordinates. It was measured by tracks of burning particles entered into the flame, and by the Pitot tube (P). The dashed line designates average radius of the fire tornado.

The tracks of luminous aluminum particles had the shape of a helical line in the domain of vortex flow. It was established by photos of the tracks that the vortex is initiated at height $z \sim 0.01 \div 0.02 \text{ m}$ (V_τ is small, Fig. 3). At a height of $0.08 \div 0.1 \text{ m}$, it becomes stable till $z = 0.6 \div 0.8 \text{ m}$, and then the diffusion combustion terminates.

Table 3. Velocity components of burning products in a fire tornado measured by different ways

| Type of the unit | Combustible material | Velocity, m/sec | | | Coordinates, 10^{-2} m | | Method of measuring |
|---------------------------|----------------------|-----------------|-------|-------|----------------------------------|------|---------------------|
| | | V_τ | V_z | V_r | x | z | |
| Swirling of the base | Oil | 1.7 | — | — | 2.0 | 5.0 | Pitot tube |
| | | 0.70 | 1.5 | — | 1.0 | 5.3 | Tracks |
| | | 0.85 | 2.9 | — | 1.1 | 10.1 | |
| Swirling from above | Large fragments | 1.40 | — | — | 2.0 | 5.0 | Pitot tube |
| | Oil | 1.30 | — | — | 2.0 | 5.0 | Tracks |
| | | 0.75 | 1.4 | — | 1.0 | 5.0 | |
| | | 0.25 | — | — | 1.0 | 2.0 | |
| | | 0.10 | — | — | 3.5 | 1.0 | |
| | | 0.70 | 2.2 | — | 2.5 | 8.0 | |
| | | 0.75 | 3.1 | — | 1.5 | 10.2 | |
| | | 0.80 | 3.0 | — | 1.0 | 10.0 | |
| | | — | — | -0.20 | 4.0 | 2.0 | Hot-wire anemometer |
| | | — | — | -0.15 | 5.0 | 2.0 | |
| | | — | — | -0.10 | 6.0 | 2.0 | |
| | — | — | -0.30 | 4.0 | 10.0 | | |
| Base in a horizontal flow | Forest combustibles | — | — | -0.25 | 5.0 | 10.0 | Pitot tube |
| | | — | — | -0.20 | 6.0 | 2.0 | |
| | | 1.8 | — | — | 2.0 | 5.0 | |
| | | 1.4 | — | — | 2.0 | 7.0 | |

Note. For all the experiments, height of fire tornados varied in time within $0.4 \div 1.0 \text{ m}$.

This fact can be explained by an inflow of air mass from the space surrounding the fire tornado, what is necessary for combustion ($15 \text{ m}^3/\text{kg}$ for oil, $5\text{--}8 \text{ m}^3/\text{kg}$ for timber) at $z < 0.02\text{--}0.08$. When $z > h_c$, combustion terminates due to insufficient concentration of combustible gases. Regardless of the way of swirling the gas flow (from bottom, from above, from the side), the fire tornado is formed at the rotation frequency of the gas f between 1.1 and 1.3 Hz (see Table 1). Further growth of the base rotation frequency led to the fire tornado destruction.

The effect of flow swirling on the combustion time for forest combustible materials of similar masses was studied. The combustibles were burned with swirling of the flow and without it. The results of measurements are presented in Table 4.

Table 4. Combustion time τ_0 on the free surface and in the swirled flow

| Experiment conditions | Time of combustion τ_0 , sec | Notes |
|---|-----------------------------------|--|
| Without swirling | 45.0 | — |
| | 43.0 | — |
| | 44.0 | — |
| With swirling of the flow, $f = 1.3 \text{ Hz}$ | 39.0 | Incomplete combustion at the edge of the base, prolonged combustion in the fire seat |

It was established that combustion time is by 10% less in a swirled flow than in the absence of swirling. This is explained by an increase of diffusion combustion velocity due to the ingress of oxygen from the surrounding medium. This, as well as the presence of the radial component of the flow velocity, demonstrates that the combustion process in the fire tornado is maintained by the ingress of an oxidizer from the surrounding medium. This corresponds to the diffusion mode of combustion.

An increase of combustion rate depending on the rotation speed was also observed at other method of fire tornado simulation (swirling by an air flow at an immobile reservoir).¹⁸

4. Discussion of results

Visualization of the hydrodynamic pattern of gas flow in a fire tornado, the measurements of gas thermodynamic parameters, combustion rates, as well as their analysis permits one to describe the mechanism of fire tornado formation and evolution.

Formation of a fire tornado follows the appearance of a cone-shaped convective column formed by gaseous pyrolysis products of reagents and combustion products. This column is formed due to the effect of Archimedean forces on the burning material. Its intensity depends not on the type of combustibles (raw oil, small- and large-scale fragments, forest combustibles), but on the density of the heat flow q (close values for different ways of swirling and types of combustibles). Swirling of the

gas flow leads to appearance of centrifugal forces tending to increase the width of the torch. However, the action of the centrifugal forces is balanced by the pressure gradient directed to the near-axis zone of the column.

The influence of the pressure gradient is determined by the gas mixture temperature in the column center, decrease of this mixture density, and the density of a heat flow from the ignition source. The decrease of gas density in the near-axis zone intensifies the up-going convective flow; the linear vertical velocity increases. This process is accompanied by increase of the torch height by several times (see Fig. 2c).

The oxidizer enters the combustion zone from the surrounding medium and the combustion rate of the source somewhat increases. In the periphery of the area with the base of the fire tornado, the combustible material burns incompletely due to the oxidizer deficiency. Therefore, the combustion process in the fire tornado has a diffusion character.

Formation and evolution of the fire tornado do not depend on the way of swirling but are defined by the appearance of a moment of force supporting the gas swirling.

The simulated fire tornado is less stable than the tornado vortex. The values of swirling parameters and base slope angle are within a rather narrow range of variations. This probably is caused by the necessity of mixing the pyrolysis products with atmospheric oxygen and by high values of temperature gradients in the fire tornado as compared with tornado vortices. Rotational frequency of the fire tornado keep a conservative value $f = 1.1\text{--}1.3 \text{ Hz}$ in all experiments. For $f > 1.3 \text{ Hz}$, the fire tornado decays, i.e., the existence of the fire tornado can be referred to phenomena of unstable burning. The centrifugal force, resulting from rotation, must be equalized by a force appearing due to pressure decrease, caused by a decrease of gas density at the fire tornado axis. Besides, formation of the fire tornado is influenced by forces of friction and gravity. It means that formation and evolution of the fire tornado are defined by action of four forces: buoyancy, gravity, friction, and the force that swirls the vortex.

The dimensionless criterion characterizing the rotational motion of particles in the fire tornado F is defined by the relation⁴

$$F = \nu h_c V_z / \Gamma^2, \quad (1)$$

where ν is the coefficient of gas kinematic viscosity in the fire tornado; $\Gamma = 2\pi r V_\tau$ is the velocity circulation.

The dimensionless Ostrogradsky criterion Os , which is used in descriptions of convective flows,²⁰ is introduced to estimate the power of heat release from the combustibles:

$$Os = \frac{Q(2r)^2}{\lambda T_0}, \quad Q = \frac{2}{S} \int_0^r q dy, \quad (2)$$

where Q is the spatial heat release; S is the area of the combustion surface; q is the measured density of the heat flow at a height of 10^{-2} m; λ is the heat conductivity of the medium.

The criteria F and Os were computed from the measured values of fire tornado height $h_c = 0.4 \div 1.0$ m, $T_0 = 900 \div 1200$ K, velocities V_z and V_τ at a height of 0.1 m (the height at which formation of the fire tornado begins), the fire tornado radius by the results of photo records. The coefficient of kinematic viscosity $\nu = (2.4 \div 4.1) \cdot 10^{-4}$ m²/sec was taken from Ref. 10.

The computed criteria F and Os are presented in Table 5.

Table 5. Dimensionless similarity criteria for different ways of simulation

| Type of the unit | F | Os |
|---------------------------|------|------|
| Swirling of the base | 0.67 | 9.22 |
| Swirling from above | 0.74 | 7.96 |
| Base in a horizontal flow | 0.76 | 9.34 |

Compare results obtained in laboratories with characteristics of natural fire tornados.¹ The dimensionless combination h_c/r was $20 \div 30$ in the experiments. When the radius of the fire tornado increases to 100–200 m, the tangential velocity at the periphery V_τ increases to 80–160 m/sec, i.e., to values, which are close to the natural. Therefore, the geometric and hydrodynamic similarities are observed.

The closeness of the similarity criteria ($F = idem$, $Os = idem$) for different ways of the fire tornado generation demonstrates that this process does not depend on the way of swirling and the chosen dimensionless values are similarity criteria for the problem under solution.

Using the condition of local mechanical equilibrium between the fire tornado and the rotating platform,¹³ as well as the experimental results obtained in Refs. 14 and 15, we could obtain a semi-empirical formula for the critical (equilibrium) rotational speed of the platform, at which the fire tornado takes place:

$$f = a_* \left(\frac{2gh_c(T_0 - T_e)}{T_e} \right)^{0.5} r^{-1}. \quad (3)$$

Here T_e is the temperature of the surrounding medium; a_* is the empirical constant; g is the acceleration due to the gravity.

As follows from analysis of Eq. (3), the value f grows with increase of the height h_c and decreases with increase of r under otherwise equal conditions. This agrees with the a priori physical considerations and experimental data.

The formula (3), up to the constant a_* , coincides with the formula obtained in Refs. 13–15. Table 6 presents the estimates for the value a_* . The average value of a_* is $0.8 \cdot 10^{-2} \pm 0.45 \cdot 10^{-2}$.

Table 6. Estimates of the constant a_* and measurement errors δa_* determined from measurements of rotational frequency f , gas temperature at the axis, and fire tornado radius at a height of 0.1 m

| f , Hz | T_e , K | T_0 , K | r , 10^{-2} m | h_c , m | a_* , 10^{-2} | $\pm \delta a_*$, 10^{-2} |
|----------|-----------|-----------|-------------------|-----------|-------------------|------------------------------|
| 1.1 | 300 | 927 | 2.4 | 0.47 | 0.602 | |
| 1.2 | 300 | 1008 | 2.6 | 0.59 | 1.365 | 0.45 |
| 1.3 | 300 | 1190 | 2.8 | 0.69 | 0.575 | |

The study of conditions for appearance and stable combustion, determination of dimensionless similarity criteria, which describe the hydrodynamic and thermal phenomena in similar structures of different sizes make it, in principle, possible to apply passive and active (with radiation sources) optical methods to measuring parameters of actual fire tornados by results of studying in laboratory conditions.

Conclusions

Fire tornados were generated in a laboratory by several independent ways. Experiments demonstrated that the fire tornado can arise at all types of interaction between the atmospheric whirlwind and the seat of fire, at the rotation frequency of the base $f = 1.1 \div 1.3$ Hz. The fire tornado consisted of a combustion center, convective column, and column-shape cloud of combustibles.

A typical sign of appearance of the fire tornado is rapid growth of flame torch height. This is explained by an increase of the inflow of an oxidizer, appearance of a column-shape front of diffusion combustion of gaseous pyrolysis products, and local equilibrium of the centrifugal force and external pressure force. Analysis of tracks of aluminum particles demonstrates that trajectories of heated particles of combustion products look like helix lines with the varying radius of curvature over the fire seat.

It was established that the stationary state of fire tornados slightly depends on the ways of their formation, realized in the experiments, as well as on the type of combustibles, used in the work.

In a particular case of combustion of a liquid fuel, the experimental data qualitatively agree with the results of the analytical study.^{13–15}

Acknowledgements

This work was supported by the Russian Foundation for Basic Research, Project No. 08-01-00496.

References

- G.F. Carrier, F.E. Fendell, and P.S. Feldman, *Teploperedacha* **107**, No 1, 16–25 (1985).
- A.M. Grishin, *Mathematical Simulation of Forest Fires and New Ways to Fight with Them* (Nauka, Novosibirsk, 1992), 407 pp.
- Yu.A. Gostintsev and A.M. Ryzhov, *Izv. Ross. Akad. Nauk, Mekh. Zhidk. Gaza*, No. 6, 52–61 (1994).

4. L. Bengtsson and J. Lighthill, eds., *Intense Atmospheric Vortices* (Springer-Verlag, New York, 1982).
5. V.V. Nikulin, *Prikl. Mekh. Tekh. Fiz.* **33**, No. 4, 42–47 (1992).
6. V.V. Nikulin, *Prikl. Mekh. Tekh. Fiz.* **36**, No. 2, 81–87 (1995).
7. V.L. Sennitskii, *Vestnik NGU*, Issue 1, 103–106 (2001).
8. S.V. Alekseenko, P.A. Kuibin, and V.L. Okulov, *An Introduction to the Theory of Concentrated Vortices* (Institute of Thermophysics, Novosibirsk, 2003), 504 pp.
9. B.M. Bubnov, *Izv. Ross. Akad. Nauk, Ser. Fiz. Atmos. Okeana* **33**, No. 4, 434–442 (1997).
10. V.P. Samsonov, *Spontaneous Vortex Structures in a Flame* (Tomsk University, Tomsk, 2003), 124 pp.
11. A.Yu. Snegirev, J.A. Marsden, J. Francis, and G.M. Makhviladze, *Int. J. Heat and Mass Transfer* **47**, Nos. 12–13, 2523–2539 (2004).
12. A.M. Grishin, S.V. Petrin, and L.S. Petrina, *Simulation and Prediction of Catastrophes*, Part 3 (Tomsk University, Tomsk, 2006), 576 pp.
13. A.M. Grishin, *Ekol. Sist. Prib.*, No. 6, 50–51 (2006).
14. A.M. Grishin, A.N. Golovanov, and Ya.V. Sukov, *Dokl. Ross. Akad. Nauk* **395**, No. 2, 196–198 (2004).
15. A.M. Grishin, A.N. Golovanov, A.A. Kolesnikov, A.A. Strokatov, and R.Sh. Tsvyk, *Dokl. Ross. Akad. Nauk* **400**, No. 5, 618–620 (2005).
16. A.M. Grishin, V.M. Sazanovich, A.A. Strokatov, and R.Sh. Tsvyk, *Atmos. Oceanic Opt.* **19**, No. 12, 935–939 (2006).
17. A.M. Grishin, A.N. Golovanov, V.V. Reino, V.M. Sazanovich, A.A. Strokatov, R.Sh. Tsvyk, and M.V. Sherstobitov, *Atmos. Oceanic Opt.* **20**, No. 3, 215–219 (2007).
18. A.M. Grishin, V.V. Reino, V.M. Sazanovich, R.Sh. Tsvyk, and M.V. Sherstobitov, *Atmos. Oceanic Opt.* **21**, No. 2, 136–141 (2008).
19. A.M. Grishin, *Ekol. Sist. Prib.*, No. 6, 52–56 (2007).
20. O.G. Martynenko and Yu.A. Sokovishin, *An Introduction to the Theory of Free Convection Heat Exchange* (Leningrad University, Leningrad, 1982), 224 pp.